Catalysts for direct H_2O_2 synthesis taking advantage of the high H_2 activating ability of Pt: Kinetic characteristics of Pt catalysts and new additives for improving H_2O_2 selectivity

Supporting Information

Takashi Deguchi[a], Hitoshi Yamano[b,d], Sho Takenouchi[c,d] and Masakazu Iwamoto[a]

[a] Research and Development Initiative, Chuo University, 1-13-27 Kasuga, Bunkyo-ku, Tokyo 112-8551, Japan.

[b] Chemical Resources Laboratory, Tokyo Institute of Technology, 4259-R1-5 Nagatsuta, Midori-ku, Yokohama 226-8503, Japan

[c] Tokyo Ohka Kogyo Co., Ltd., 1590 Tabata, Samukawa-machi, Koza-gun, Kanagawa 253-0114, Japan.

[d] Tanaka Kikinzoku Kogyo K.K., 2-14 Nagatoro, Hiratsuka, Kanagawa 254-0021, Japan.

Details of experimental procedure and data processing

1. Experimental procedure

The reaction was performed in a 300 ml flat-bottom separable flask made of Pyrex glass with an inner diameter of 80 mm that was equipped with a cross-shaped magnetic rotor with a length of 50 mm and a height of 15 mm. The rotation rate during the reaction was 1,200 rpm, and the gas-liquid contact was primarily due to high-rate agitation. Prescribed amounts of catalyst and water were introduced into the flask. H_2 gas was flowed at a rate of 20 sccm at 303 K into the reactor for 40 min to activate the catalyst. Then, N_2 gas was introduced (50 sccm, 10 min) to purge the H_2 gas, and the additive(s) was added in the form of an aqueous or methanol solution. Finally, the volume of the solution was adjusted to 300 ml. After sufficient displacement with N_2 (50 sccm, 10 min), a mixture consisting of H_2, O_2 and N_2 gases was continuously passed into the reactor at ambient pressure. The flow rate of each gas was regulated by a high precision mass flow controller, and calibrated using a soap-film flow meter before the reaction. The outlet gas composition was analyzed periodically (every 10 minutes) by gas chromatography using N_2 as an internal standard to determine the consumption rates of H_2 and O_2. The reaction temperature was maintained at 303 K. The ambient

pressure p_a (kPa) and the ambient temperature T_a (K), were measured at the start and the end of the reaction, and the averages were taken. Before and after the reaction, gas chromatogram of the feed gas was acquired off line every three times, and the relative sensitivity coefficients of H_2, O_2 and N_2 were determined by averaging. At the same time as the final gas sampling, the reaction mass was sampled for determination of the H_2O_2 concentration using a UV-Vis absorption method with a titanium sulfate solution.

Fig. S1 shows a typical time course of the outlet gas composition. Here x_{H2}, x_{O2} and x_{N2} represent the mole ratios of H_2, O_2 and N_2, respectively ($x_{H2} + x_{O2} + x_{N2} = 1$). The outlet flow rates of H_2 and O_2, f_{H2} and f_{O2}, are calculated by Eqs. (1) and (2), in which f_{N2} is the flow rate of N_2 (sccm). The total flow rate, f_{total}, is represented by Eq. (3), in which the vapor pressure of H_2O is neglected for simplicity. The partial pressures of H_2 and O_2 in the reactor, p_{H2} and p_{O2}, were calculated from the gas composition taking into accounts of the vapor pressure of H_2O at 303 K as shown by Eqs. (4) and (5), in which Δp and p_{H2O} are the pressure drop caused by the outlet piping and the vapor pressure of H_2O at 303 K (kPa), respectively.

$$f_{H2} = f_{N2}(x_{H2}/x_{N2}) \quad (1)$$

$$f_{O2} = f_{N2}(x_{O2}/x_{N2}) \quad (2)$$

$$f_{total} = f_{H2} + f_{O2} + f_{N2} \quad (3)$$

$$p_{H2} = (p_a + \Delta p - p_{H2O})x_{H2} \quad (4)$$

$$p_{O2} = (p_a + \Delta p - p_{H2O})x_{O2} \quad (5)$$

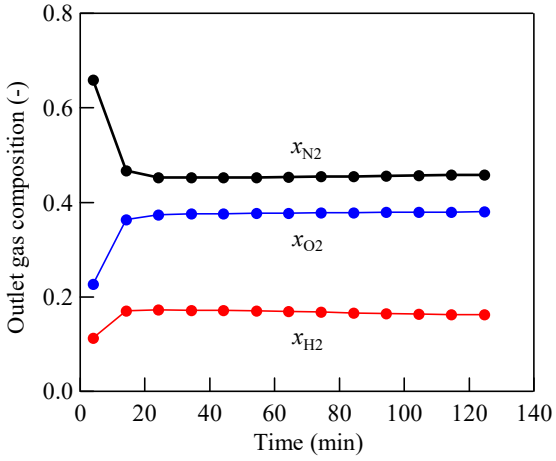

Fig. S1. Typical time course of outlet gas composition in the H_2-O_2 reaction over Pd-PVP catalyst in water in the presence of H_2SO_4 and NaBr (corresponding to the experiment using Pd-PVP shown in Fig. 1 in the main paper). Pd 8.33 mg L^{-1}, H_2SO_4 0.01 N, NaBr 0.001 N, gas feed: H_2 10.03; O_2 18.69; N_2 19.96 sccm, p_{H2} 17-16 kPa, p_{O2} 37 kPa, 303 K, 1,200 rpm.

2. Data handling for the initial unsteady state of the reaction

As shown in Fig. S1, the gas composition at the outlet reached a stationary state after some induction period. The gas phase volume in the reactor was therefore set as small as possible in order to minimize the induction period. The reaction during the induction period was evaluated as follows. Fig. S2 picks up the time course of H_2 mole ratio during the initial 60 min from Fig. S1. One can understand that the stationary state was attained after the third point, and thereafter the composition was assumed to vary linearly with time. The calibrated reaction start time, t_0, was estimated by Eq. (6), in which v_1 (= 188.5 ml) and v_2 (= 31.6 ml) are the gas phase volume in the reactor and the piping volume from the reactor to the gas sampler of the gas chromatograph, respectively. The areas of S_1 and S_2 in the figure was essentially equal when t_0 is determined by Eq. (6).

$$t_0 = \{(v_1/f_{\text{total}})(273/303) + (v_2/f_{\text{total}})(273/T_a)\}(p_a/101.3) \qquad (6)$$

Eq. (6) means the average retention time of the feed gas (no reaction) in the dead volume from the inlet of the reactor to the inlet of the gas sampler of the gas chromatograph, and therefore t_0 is affected by the reaction to some extent. However, both of the composition of H_2 in the feed gas and its conversion are relatively low, and the conversion of O_2 is further lower, the influence of the reaction practically negligible. In the case of the Pt/C-H_2SO_4-NaBr system shown in Fig. 12 (an example affording the highest reaction rate), the total gas feed rate was 48.69 sccm (H_2 10.20, O_2 18.38, N_2 19.82) and the average outlet gas flow rate was 42.69 sccm (H_2 6.58, O_2 16.29, N_2 19.82), 12 % lower than the feed rate. Because the values of t_0 were around 5 min, the deviation

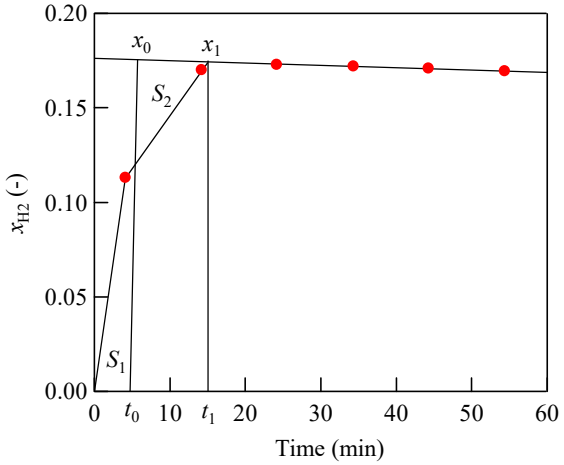

Fig. S2. Enlarged view of the time course of H_2 mole ratio of Fig. S1. The point (t_1, x_1) is the intersection of the two straight lines; one by three-point linear approximation using the fourth, fifth and sixth plots, and the other through the first and the second plots.

corresponds to 0.6 min, and the ratio to the total reaction time (120 min) is only 0.5 %.

On the other hand, the reaction curve was extrapolated to time t_0 by three-point linear approximation using the fourth, fifth and sixth plots, and x_0, the calibrated H_2 mole ratio at t_0, was determined. The calibrated O_2 and N_2 mole ratios at t_0 were also determined in the same way. Thus, the reaction curves were calibrated as if the reaction was initiated at t_0 steadily from the beginning. The reaction time for the n'th sampling time, t_{n-1}, was defined as the time subtracting t_0 from the actual sampling time, and the redefined t_0 was set at 0. The values of the mole ratios at the second and the third sampling times, were determined on the extrapolated straight lines. For $n > 4$, the values of gas composition were not varied.

3. Analyses of H_2 consumption and H_2O_2 formation based on the mass balances of the gas components

The reaction rates of H_2 and O_2, r_{H2} and r_{O2} (mmol L^{-1} h^{-1}), were calculated by Eqs. (7) and (8), respectively.

$$r_{H2} = (f^{\circ}_{H2} - f_{H2}) \times 60/22.4/0.300 \quad (7)$$

$$r_{O2} = (f^{\circ}_{O2} - f_{O2}) \times 60/22.4/0.300 \quad (8)$$

From the material balance of H_2 and O_2, r_{H2} and r_{O2} are related to the rates of H_2O_2 and H_2O concentration changes, $d[H_2O_2]/dt$ and $d[H_2O]/dt$, by Eqs. (9) and (10), in which change in the volume of the reaction mass is neglected.

$$r_{H2} = d[H_2O_2]/dt + d[H_2O]/dt \quad (9)$$

$$r_{O2} = d[H_2O_2]/dt + (1/2)d[H_2O]/dt \quad (10)$$

Eqs. (9) and (10) can be transformed to Eqs. (11) and (12).

$$d[H_2O_2]/dt = 2r_{O2} - r_{H2} \quad (11)$$

$$d[H_2O]/dt = 2r_{H2} - 2r_{O2} \quad (12)$$

$d[H_2O_2]/dt$ was calculated at each sampling time. The H_2O_2 concentration in the reaction mass, $[H_2O_2]$ (mmol L^{-1}) was calculated by numerical integration of Eq. (11) at each sampling point. The accumulated H_2 consumption, $\int r_{H2}dt$ (mmol L^{-1}), was also calculated by numerical integration. The effective H_2O_2 selectivity, S_e (-), can be calculated by Eq. (13) at each sampling point.

$$S_e = [H_2O_2]/\int r_{H2}dt \quad (13)$$

The actual concentration of H_2O_2 at the final sampling time, $[H_2O_2]_{det}$ was

determined using a UV-Vis absorption method with a titanium sulfate solution. Based on $[H_2O_2]_{det}$, another expression of the effective H_2O_2 selectivity at the final sampling time, $(S_e)_{det}$, was given by Eq. (14), in which $(\int r_{H2}dt)_{fin}$ denotes the overall H_2 consumption.

$$(S_e)_{det} = [H_2O_2]_{det}/(\int r_{H2}dt)_{fin} \qquad (14)$$

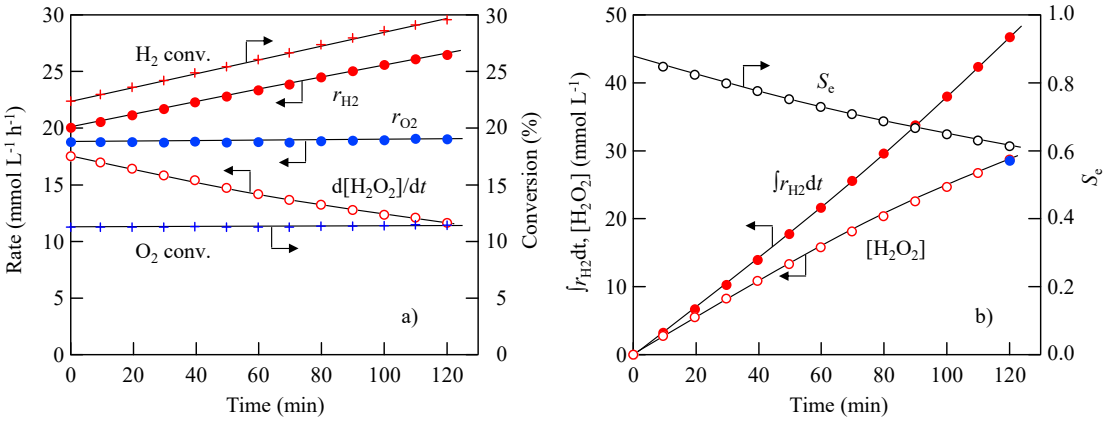

Fig. S3. Time course of the H_2O_2 reaction derived from the experimental data shown in Fig. S1. The blue solid circle in Fig. S3b shows $[H_2O_2]_{det}$.

Fig. S3 shows the time course of the H_2-O_2 reaction derived from the experimental data shown in Fig. S1. r_{H2} gradually increased with time, and the H_2 conversion increased correspondingly, whereas r_{O2} and the O_2 conversion was almost constant. The increase in r_{H2} is a phenomenon characteristic of the Pd-PVP catalyst in the presence of H^+ and Br^-, and the reason was described in our previous paper [1]. That is, we concluded that the reaction proceeded via Langmuir-Hinshelwood mechanism, in which H_2, O_2 and H_2O_2 equilibratedly adsorbed on the Pd surfaces, and dissociatively adsorbed H species reacted with adsorbed O_2 and H_2O_2 species in the rate-determining steps. According to this mechanism, r_{H2} (and also H_2 conversion) could increase along with accumulation of H_2O_2 while r_{O2} was constant (at constant p_{O2}). On the other hand, $d[H_2O_2]/dt$ decreased with time due to the increasing rate of the H_2O_2 destruction exhibited by Eq. (4) in the main paper. Although the rate of H_2O_2 accumulation decreased with time, H_2O_2 was accumulated with time. S_e decreased with time. The $[H_2O_2]_{det}$ in Fig. S3b agreed excellently with $[H_2O_2]_{fin}$, the calculated H_2O_2 concentration at the final sampling point, (28.6 and 28.7 mmol L^{-1}), as shown with a blue circle. Fig. S4 shows all of the plots of $[H_2O_2]_{det}$ against $[H_2O_2]_{fin}$ for the

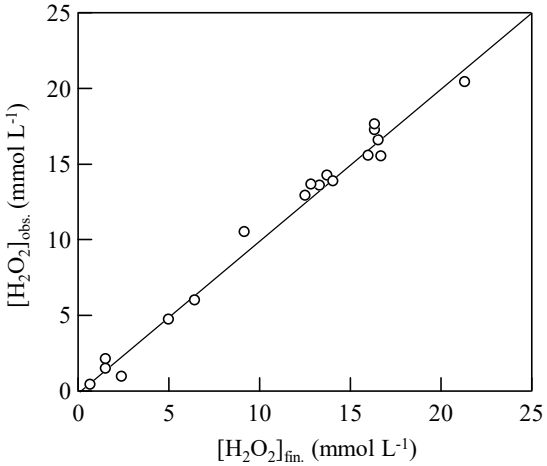

Fig. S4. Relationship between $[H_2O_2]_{fin.}$ and $[H_2O_2]_{obs.}$ related to the experiments shown in Figs. 11 and 12.

experiments of Figs. 11 and 12 in the main paper, indicating the very good correlation ($R^2 = 0.986$). These findings revealed that the present data processing was reasonable and acceptable for kinetic discussion.

4. Rate analyses of the concurrent and the consecutive reactions

We proposed Eq. (15) (Equation (4) in the main paper) for kinetic analysis of the H_2O_2 synthesis. Here, S_f, k_d and [Cat] represent H_2O_2 formation selectivity, H_2O_2 destruction rate constant and catalyst concentration, respectively. S_f and k_d include the terms of H_2 and O_2 partial pressures, p_{H2} and p_{O2}. Determination of S_f and k_d according to Eq. (15) was performed as described in our previous paper [2, 3]. Integration of Eq. (15), assuming that S_f is constant, followed by the subsequent rearrangement of the resulting equation affords Eq. (16), in which Σ_1 and Σ_2 are defined as $\Sigma_1 = \int r_{H2} dt$ and $\Sigma_2 = \int [H_2O_2] dt$, respectively. When linear relationship holds between $\Sigma_1/[H_2O_2]$ and $\Sigma_2/[H_2O_2]$, the values of S_f and k_d can be calculated from the intercept and the slope of the correlation line. Actually the integrations were carried out by the trapezoidal method.

$$d[H_2O_2]/dt = r_{H2}S_f - k_d[H_2O_2][Cat] \quad (15)$$

$$\Sigma_1/[H_2O_2] = 1/S_f + (k_d[Cat]/S_f)\ \Sigma_2/[H_2O_2] \quad (16)$$

Fig. S5 shows the plots of $\Sigma_1/[H_2O_2]$ vs. $\Sigma_2/[H_2O_2]$ with respect to the experiments shown in Fig. 12 in the paper. A fine linear relationships can be seen, and the values of S_f and k_d[Cat] are determined as shown in the figure.

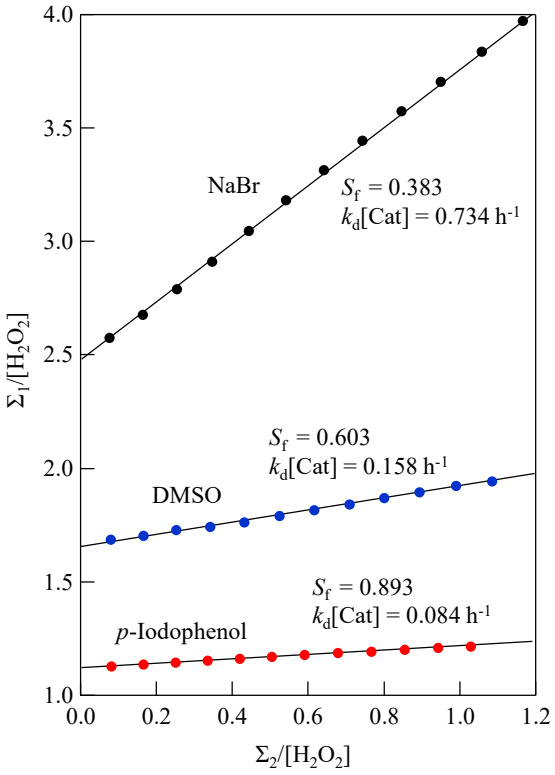

Fig. S5. Plots of $\Sigma_1/[H_2O_2]$ against $\Sigma_2/[H_2O_2]$ for the experiments shown in Fig. 12 in the paper.

5. Effectiveness and limits of the present methods

The above-mentioned experimental and calculation methods for H_2 consumption and H_2O_2 formation based on the mass balances of the gas components have some significant advantages compared to the conventional methods, in which $[H_2O_2]$ is determined by quantitative analysis. First is that sampling of the reaction mass during the reaction time is unnecessary. Sampling of the reaction mass disturbs the reaction conditions (the amount of the reaction mass including the catalyst, and the volume of the gas phase), which makes the kinetic analysis of the reaction complicated. Second is that more frequent analysis of the reaction is available. The number of the sampling times is limited in the cases of the conventional methods, because a drastic change in the volume of the reaction mass as well as that of the gas phase causes a change in the gas-liquid contact, which is fatal for kinetic analyses.

On the other hand, the present method has also some weaknesses. First is that it needs precise gas feed controls and precise analysis of gas composition. However, the former is the same in the cases of the conventional methods, and the latter is not difficult to be executed by using the modern gas chromatograph. Second is that this method can be applied only when the rate of H_2O_2 accumulation, $d[H_2O_2]/dt$, is satisfactorily large. When $d[H_2O_2]/dt$ is small, the error of each terms in Eq. (11) is

enlarged by subtraction and the accuracy of the analysis becomes lower. On such catalysts, $[H_2O_2]_{det}$ and $(S_e)_{det}$ should be adopted similar to the conventional methods.

References

[1] T. Deguchi, H. Yamano, M. Iwamoto, J. Catal., 287 (2012) 55.
[2] T. Deguchi, M. Iwamoto, Ind. Eng. Chem. Res., 50 (2011) 4351.
[3] T. Deguchi, H. Yamano, M. Iwamoto, Catal. Today, 248 (2015) 80.